scientific reports

Check for updates

OPEN

Sigma1R restores mitochondrial energy metabolism via the IRE1α/XBP1 pathway

Wei Yan[1,2], Tongyuan Deng[1], Da Huang[1], Bailu Deng[3], Hong Ling[4] & Zhile Li[1,2]✉

To investigate the role of Sigma1 receptor (Sigma1R) in mitochondrial energy metabolism remodeling in atrial myocytes, elucidate the associated molecular mechanisms, and evaluate its therapeutic potential in atrial fibrillation (AF). HL-1 atrial myocytes were subjected to tachypacing at 5 Hz for 24 h to establish an AF model. Lentiviral vectors were used to modulate Sigma1R and IRE1α expression. Cell viability was assessed by CCK-8 assay, apoptosis by Annexin V-FITC/PI staining and flow cytometry, mitochondrial function by TMRE staining for membrane potential, MitoSOX Red for reactive oxygen species (ROS) detection, and ATP assays. Calcium dynamics were measured using Fura-2/AM and Fluo-3/AM imaging. Protein expression was analyzed by Western blot, and subcellular localization was confirmed by fluorescence in situ hybridization (FISH). Tachypacing induced significant damage in atrial myocytes, including a 32.16% apoptosis rate, decreased Sigma1R expression, mitochondrial swelling, a 38% reduction in ATP levels, a 37% increase in mitochondrial ROS, and a 122% increase in cytosolic calcium compared to control cells. Overexpression of Sigma1R significantly mitigated these effects: cell viability increased by 55% ($P < 0.001$), apoptosis was reduced by 55% ($P < 0.01$), ATP levels were restored to 84% of control values ($P < 0.01$), and mitochondrial ROS decreased by 55% ($P < 0.05$). Mechanistically, Sigma1R overexpression normalized calcium homeostasis, reducing cytosolic calcium to 134 ± 11 nM from 218 ± 16 nM in the AF group ($P < 0.01$) and suppressed pathological expansion of endoplasmic reticulum-mitochondria contact sites. The activation of the IRE1α/XBP1 pathway was inhibited by Sigma1R, as evidenced by reductions in IRE1α, phosphorylated IRE1α, and XBP1s protein levels by 39–47% ($P < 0.05$). Conversely, IRE1α overexpression abrogated the protective effects of Sigma1R, leading to a 22% increase in apoptosis ($P < 0.01$) and exacerbating mitochondrial and calcium dysfunction. Sigma1R protects atrial myocytes from tachypacing-induced injury by enhancing mitochondrial function, reducing oxidative stress, and regulating calcium homeostasis at mitochondria-associated membranes, primarily through inhibition of the IRE1α/XBP1 pathway. These findings highlight Sigma1R as a promising therapeutic target for mitigating mitochondrial remodeling in AF.

Keywords Atrial fibrillation, Sigma1 receptor, Mitochondria, IRE1α/XBP1 pathway, Calcium homeostasis

Atrial fibrillation (AF), the most prevalent supraventricular arrhythmia, is characterized by rapid, irregular atrial contractions that impose a substantial burden on global cardiovascular health. This condition is intricately linked to heightened morbidity and mortality, with well-documented associations to ischemic stroke, myocardial infarction, heart failure, renal dysfunction, and cognitive decline[1,2]. Current therapeutic strategies-encompassing rate control, rhythm control, anticoagulation, and upstream interventions-are hindered by limitations such as bleeding risks, proarrhythmic effects, and suboptimal long-term efficacy, underscoring the critical need for mechanistically novel therapeutic targets[3,4].

A growing body of evidence highlights the central role of mitochondrial energy metabolism remodeling in atrial myocytes as a pivotal driver of AF progression. This remodeling entails dysfunctional mitochondrial bioenergetics, perturbed high-energy phosphate homeostasis, and altered substrate utilization, collectively culminating in structural and electrophysiological abnormalities that facilitate arrhythmogenesis[5,6].

[1]Department of Cardiovascular Medicine, Affiliated Hospital of Youjiang Medical University for Nationalities, Baise City, Guangxi Province, China. [2]Laboratory of the Atherosclerosis and Ischemic Cardiovascular Diseases, Affiliated Hospital of Youjiang Medical University for Nationalities, Baise City, Guangxi Province, China. [3]Department of Cardiovascular Medicine, Wuzhou People's Hospital, Wuzhou City, Guangxi Province, China. [4]Graduate School, Youjiang Medical University for Nationalities, Baise City, Guangxi Province, China. ✉email: googlee0220@163.com

Mechanistically, mitochondrial dysfunction in AF is characterized by reduced ATP production, depolarized mitochondrial membrane potential, and enhanced sarcolemmal K-ATP channel activity, which collectively disrupt electrical conduction homogeneity and promote reentrant circuit formation[7]. These observations position mitochondrial homeostasis as a critical nodal point for therapeutic intervention.

The Sigma1 receptor (Sigma1R), an endoplasmic reticulum (ER)-resident chaperone, has emerged as a key modulator of cardiovascular health, particularly in maintaining organelle crosstalk at mitochondria-associated membranes (MAMs)-specialized microdomains enabling bidirectional communication between the ER and mitochondria[8,9]. Genetic and pharmacological studies have demonstrated that Sigma1R deficiency disrupts ER-mitochondria contact sites, impairs Ca^{2+} transfer to mitochondria, and exacerbates mitochondrial dysfunction[8]. Clinically, Sigma1R activation mitigates atrial remodeling and reduces AF susceptibility, whereas its inhibition promotes arrhythmogenic substrate formation[10]. Despite these advancements, the precise molecular mechanisms by which Sigma1R orchestrates mitochondrial energy metabolism in atrial myocytes-specifically through regulation of ER-mitochondria Ca^{2+} dynamics-remain incompletely understood.

A critical interface for Sigma1R-mediated signaling lies in its interaction with IRE1α, a sensor of ER stress and a central component of the unfolded protein response (UPR). IRE1α coordinates adaptive signaling between the ER, mitochondria, and nucleus to restore cellular homeostasis, with dysregulation of the IRE1α/XBP1 pathway implicated in multiple cardiac pathologies[11]. Notably, recent work has shown that Sigma1R activation protects against cardiac fibrosis by attenuating IRE1α-mediated UPR overactivation[12,13]. Given the pivotal role of ER-mitochondria Ca^{2+} flux in regulating mitochondrial bioenergetics and the established crosstalk between Sigma1R and IRE1α, we hypothesize that Sigma1R modulates atrial myocyte mitochondrial metabolism during AF by suppressing IRE1α/XBP1-dependent dysregulation of MAM-localized Ca^{2+} transport complexes.

This study aims to delineate the role of Sigma1R in mitochondrial energy metabolism remodeling within the context of AF, with a specific focus on its impact on mitochondrial structure, oxidative stress, and Ca^{2+} homeostasis in atrial myocytes. By interrogating the mechanistic link between Sigma1R and the IRE1α/XBP1 pathway, we seek to uncover novel insights into AF pathogenesis and validate Sigma1R as a promising therapeutic target for interrupting the vicious cycle of mitochondrial dysfunction and arrhythmogenesis.

Methods

HL-1 cardiomyocyte cell culture and tachypacing

HL-1 atrial cardiomyocytes, originating from adult mouse atria, were obtained from Wuhan Suuncell Technology (China) and maintained in DMEM/F12 medium (Wuhan Pricella Biotechnology, China) supplemented with 10% FBS (Suzhou ExCell Biotechnology, China), and penicillin streptomycin solution (Beyotime, China). The cardiomyocytes were cultured on glass coverslips at 37 °C in a 5% CO_2 environment.

HL-1 atrial cardiomyocytes were subjected to normal pacing (1 Hz) or tachypacing at 10 V/cm pulse for different hours utilizing the YC-2 programmed electrical stimulation instrument (Chengdu Instrument Factory, China) with or without lentiviral expression vectors[14].

Lentiviral construction and transduction

The Sigma1R and IRE1α lentiviral expression vectors were constructed by Shanghai Sangon Biotech (China). The CDS sequence of Sigma1R or IRE1α was sub-cloned into the lentiviral expression vector pLV-Puro. The sh-IRE1α lentiviral vectors were constructed by Shanghai Sangon Biotech (China) and were used to knock down the IRE1α expression. The negative control lentiviral vector containing nonsilencing short hairpin RNA (shRNA) was used. The shRNA sequences are described in Supplementary Table 1. HL-1 cells were plated into 6-well plates. When HL-1 cell confluence reaching 80%, cells were co-transfected with lentiviral vector (or control vector). The transfection was performed by using LipoFectamine 3000 Transfection Reagent (Thermo Fisher, USA). The transfection media were changed 8 h after transfection.

Quantitative reverse transcription polymerase chain reaction (RT-qPCR)

Total RNA was extracted by the FastPure Cell/Tissue Total RNA Isolation Kit V2 (Vazyme, China). cDNA was generated using HiScript lll 1st Strand cDNA Synthesis for RT-qPCR kit (Vazyme, China). RT-qPCR analysis was performed using the Taq Pro Universal SYBR qPCR Master Mix kit (Vazyme, China) and CFX96 Touch Real-Time PCR Detection System (Bio-Rad, USA). Relative mRNA expression was analyzed using the $2^{-\Delta\Delta Ct}$ method, with normalization to GAPDH expression. Primer sequences are shown in Supplementary Table 2.

Western blot analysis

Total protein was isolated from the HL-1 cells using RIPA lysis buffer (Beyotime, China). Protein concentrations were determined using the bicinchoninic acid assay (NCM Biotech, China). Proteins were separated using 12% SDS-PAGE gels and electro-transferred to PVDF membranes. The membranes were then blocked by rapid blocking liquid for 30 min at room temperature and incubated overnight, respectively, with primary antibodies at 4 °C. After washing with TBST three times, the membranes were incubated, respectively, with secondary antibody at 37 °C for 2 h. The dilutions and suppliers of the primary antibodies and secondary antibodies are documented in Supplementary Table 3. Protein blots were detected using a chemiluminescence kit (NCM Biotech, China) and JP-K6000 Chemiluminometer (Shanghai JiaPeng Technology, China). The protein bands were visualized with chemiluminescence ECL reagent and recorded. The signal intensity was analyzed by ImageJ software. β-Tubulin content was used to standardize sample loading.

CCK-8 assay for cell viability

HL-1 cells were seeded at a density of 2000 cells per well in 96-well plates (Corning, USA, Cat.No.3596), with 100 µL of DMEM/F12 medium (Gibco, USA, Cat.No.11320033) containing 10% fetal bovine serum (FBS, Gibco, USA, Cat.

No.10099141) per well. Experimental groups include the control group, tachypacing group, tachypacing + Sigma1R overexpression lentivirus group (OE- Sigma1R), and tachypacing + control lentivirus group (OE-NC). Following treatment, 10 μL of CCK-8 solution (Dojindo, Japan, Cat.No.CK04) was added to each well, and plates were incubated at 37 °C in a 5% CO_2 humidified atmosphere for 2 h. Absorbance at 450 nm was measured using a Flurosikan Ascent microplate fluorometer (Thermo Fisher Scientific, USA, Model: FLx800), with blank wells used for background correction. Cell viability was calculated as the ratio of experimental to control absorbance values, expressed as a percentage: $\text{Cell Viability } (\%) = (\text{OD450 experimental}/\text{OD450 control}) \times 100\%$.

FISH detection

Cells were fixed with 4% paraformaldehyde (PFA) for 15 min to preserve protein antigenicity.

Permeabilization: Treat with 0.5% Triton X-100 for 10 min, then incubated with primary antibody overnight at 4 °C. Secondary antibody labeling: Incubating with fluorophore-conjugated secondary antibody at 37 °C for 1 h (protected from light), using cross-linked secondary antibodies to minimize disruption during subsequent FISH denaturation steps. Applying 4% PFA for 10 min to immobilize protein-antibody complexes, then subjected to florence microscopy.

TMRE staining for mitochondrial membrane potential

Mitochondrial membrane potential was assessed using the TMRE Mitochondrial Membrane Potential Assay Kit (Abcam, UK, Cat.No. ab113852). Cells grown on glass coverslips (Marienfeld, Germany, Cat.No.010590) were treated and incubated with 50 nM TMRE working solution at 37 °C in the dark for 30 min to label intact mitochondria. After three washes with PBS, images were acquired using a Leica DMI8 fluorescence microscope (Leica Microsystems, Germany) with excitation at 549 nm and emission at 575 nm. Ten random fields per sample were captured, and fluorescence intensity was quantified using ImageJ software (National Institutes of Health, USA).

Flow cytometry for apoptosis detection

Cell apoptosis was evaluated using the Annexin V-FITC/PI Apoptosis Detection Kit (Thermo Fisher Scientific, USA, Cat.No. V13242). Cells (1×10^5) were collected, washed twice with cold PBS, and centrifuged at 300 × g for 5 min at 4 °C. Pellets were resuspended in 100 μL of 1 × Binding Buffer (kit-provided), followed by incubation with 5 μL Annexin V-FITC and 5 μL PI staining solution at room temperature in the dark for 15 min. Reactions were stopped by adding 400 μL of 1 × Binding Buffer, and samples were analyzed using a BD FACSCanto II flow cytometer (BD Biosciences, USA). Apoptotic cells were defined as the sum of Annexin V^+/PI^- (early apoptosis) and Annexin V^+/PI^+ (late apoptosis) populations, with three biological replicates per group.

Mitochondrial superoxide (ROS) detection

Mitochondrial superoxide levels were measured using MitoSOX Red Mitochondrial Superoxide Indicator (Thermo Fisher Scientific, USA, Cat.No.M36008). Cells seeded in 24-well plates (Greiner Bio-One, Germany, Cat.No.662160), treated and incubated with 1 mL of 5 μM MitoSOX Red in HBSS buffer (Gibco, USA, Cat. No.14025092) at 37 °C in the dark for 15 min. After three PBS washes, live-cell imaging was performed using a Leica DMI8 fluorescence microscope (excitation: 510–550 nm, emission: 570 nm). Fifteen fields per sample were analyzed, and fluorescence intensity was quantified using ImageJ, normalized to control samples.

Intracellular calcium ($[Ca^{2+}]$ i) measurement

Cytosolic calcium activity was determined using the Fura-2/AM calcium probe (Thermo Fisher Scientific, USA, Cat.No. F1221). Cells grown on glass coverslips were loaded with 2 μM Fura-2/AM (dissolved in 0.02% Pluronic F-127) in HEPES-buffered saline (HBS; 135 mM NaCl, 5 mM KCl, 1 mM $MgCl_2$, 1.8 mM $CaCl_2$, 10 mM HEPES, 10 mM glucose, pH 7.4) at 37 °C for 40 min. Loaded cells were transferred to a 0.2 mL perfusion chamber mounted on a Leica DMI8 inverted microscope (equipped with a Lambda DG-4 excitation source, Sutter Instruments, USA). Fluorescence was excited at 340 nm and 380 nm, with emission detected at 510 nm using a computer-controlled monochromator. The ratio of fluorescence intensities (F340/F380) was calculated using MetaFluor software (Molecular Devices, USA) to quantify $[Ca^{2+}]$ i changes.

ATP content assay

Intracellular ATP levels were measured using an ATP Assay Kit (Beyotime, China, Cat.No. S0026). Cells were washed with cold PBS, lysed on ice with 100 μL of cell ATP-releasing reagent (kit-provided), and centrifuged at 12,000 × g for 5 min at 4 °C. Supernatants (50 μL) were mixed with 50μL of luciferin-luciferase working solution (prepared fresh) in 96-well black plates (Corning, USA, Cat.No.3603), and chemiluminescent signals (562 nm) were detected using a Flurosikan Ascent microplate fluorometer (Thermo Fisher Scientific, USA). ATP concentration was calculated from a standard curve (0–1000 nM ATP) and normalized to protein concentration, determined simultaneously by BCA Protein Assay Kit (Beyotime, China, Cat.No. P0010), with results expressed as nmol ATP/mg protein.

Mitochondria morphology analysis

To quantify the change in mitochondrial morphology in detail, HL-1 cells were observed using electron microscopy (JEM-1400, Japan) as previous described[15] After 24 h of treatment, HL-1 cells were fixed in a cold fixative solution containing 2.5% glutaraldehyde in 0.1 M phosphate buffer (pH 7.2) and 2% paraformaldehyde in 0.1 M phosphate overnight at 4 ℃. The fixed cells were then dehydrated through a graded ethanol series and embedded in epoxy resin. Epoxy resin-embedded samples were loaded into capsules and polymerized at 38 ℃ for 12 h, followed by 60 ℃ for 48 h. Sliced sections were cut using an ultramicrotome (RMC MT-XL, USA) and

collected on a grid made of copper. Appropriate areas from thin sectioning were cut at 65 nm and stained with saturated 4% uranyl acetate and 4% lead citrate, and then examined with a transmission electron microscope at 80 kV. Representative micrographs were obtained to evaluate mitochondrial morphology in treated and control groups.

Statistical analysis

All data were expressed as mean ± SD. A one-way or two-way ANOVA, Mann–Whitney U test, and two-tailed Student's *t*-test were used to determine statistical significance. Data were analyzed using Prism 9.4.0 (GraphPad, USA). The $P < 0.05$ was considered statistically significant.

Results

Sigma1R overexpression attenuates tachypacing-induced cellular injury

To establish an *in vitro* AF model, HL-1 atrial myocytes were subjected to electrical stimulation at increasing frequencies (0–5 Hz). High-frequency stimulation (5 Hz) significantly downregulated L-type Ca^{2+} channel (LTCC) mRNA ($P < 0.01$) and protein ($P < 0.05$) expression (Supplementary Fig. 1A and B), indicating impaired Ca^{2+} influx and electrophysiological remodeling. Therefore, 5 Hz, 10 V stimulation for 24 h was selected for subsequent experiments. Under these conditions, cell viability markedly decreased and apoptosis increased to 32.16% (Supplementary Fig. 1C and D), confirming the establishment of a robust AF-like stress model. Previous studies have reported the protective effects of Sigma1R agonists in AF-related remodeling[16]. Sigma1R expression was significantly reduced in AF-treated cells compared with controls (Fig. 1A and B). To assess its functional relevance, HL-1 cells were transduced with a Sigma1R-overexpressing lentivirus (OE-Sigma1R). Sigma1R overexpression markedly reduced apoptosis by 55% relative to AF + OE-NC cells (32.59% vs. 14.65%; $P < 0.001$; Fig. 1C). Time-course analysis further demonstrated that Sigma1R conferred significant and sustained improvements in cell viability at 24, 48, and 72 h (all $P < 0.001$; Fig. 1D). Together, these findings indicate that Sigma1R overexpression provides early and durable protection against tachypacing-induced cellular damage.

Sigma1R overexpression improves mitochondrial structure and bioenergetic function

Given the localization of Sigma1R at ER–mitochondria contact sites, we next examined its role in mitochondrial integrity. Transmission electron microscopy revealed normal tubular mitochondria in the control group, whereas AF and AF + OE-NC cells displayed swollen, spherical mitochondria with substantial ultrastructural damage (Fig. 2A). Sigma1R overexpression markedly attenuated these abnormalities, restoring mitochondrial morphology and organization. Bioenergetic analyses further supported these structural improvements. Tachypacing reduced ATP levels by ~ 34% compared with controls (17.39 vs. 26.53 nM; Fig. 2B), whereas Sigma1R overexpression increased ATP content to 22.34 nM—a 35% recovery relative to AF + OE-NC cells (16.60 nM) and ~ 84% of control levels. Mitochondrial ROS increased ~ 3.7-fold in AF cells (0.843 vs. 0.180; Fig. 2C), but Sigma1R significantly reduced ROS to 0.367 (a ~ 55% decrease vs. AF + OE-NC). Similarly, tachypacing reduced mitochondrial membrane potential ($\Delta\Psi m$) by ~ 74% (0.223 vs. 0.847; Fig. 2D), whereas Sigma1R restored $\Delta\Psi m$ to 0.653 (a ~ 175% improvement), corresponding to ~ 77% of control levels. Collectively, these findings demonstrate that Sigma1R overexpression preserves mitochondrial structural integrity, restores bioenergetic function, and mitigates oxidative stress under AF-like conditions.

Given that Sigma1R resides at mitochondria-associated membranes and modulates ER–mitochondria crosstalk, we next investigated whether its effects on mitochondrial bioenergetics are mediated by alterations in MAM structure, Ca^{2+} flux, and IRE1α/XBP1 signaling.

Sigma1R restores ER–mitochondria calcium transport by normalizing MAM structure

Transmission electron microscopy revealed pronounced ultrastructural abnormalities in AF-treated cells, including swollen mitochondria and excessively elongated ER–mitochondria contact sites, consistent with pathological MAM tethering (Fig. 3A–D). Sigma1R overexpression markedly normalized these alterations, restoring mitochondrial number, reducing abnormal MAM elongation, and re-establishing physiological ER–mitochondria apposition. Functionally, AF induced substantial cytosolic calcium overload ($\Delta[Ca^{2+}]i = 218 \pm 16$ nM vs. 98 ± 8 nM in controls; $P < 0.001$), which was significantly attenuated by Sigma1R overexpression (134 ± 11 nM; $P < 0.01$; Fig. 3E–F). Consistent with this, Fluo-2/AM and Fluo-3/AM imaging showed elevated cytosolic and mitochondrial Ca^{2+} levels in AF+OE-NC cells, both of which were significantly reduced in the AF + OE-Sigma1R group (Fig. 3G–H). Treatment with the IP_3R antagonist 2-APB similarly lowered Ca^{2+} levels, supporting the involvement of ER-derived Ca^{2+} release in AF-induced calcium dysregulation. Together, these findings demonstrate that Sigma1R alleviates pathological ER–mitochondria calcium transfer by restoring normal MAM architecture and limiting excessive ER Ca^{2+} release under tachypacing stress.

Sigma1R attenuates MAM tethering by inhibiting the IRE1α/XBP1 signaling axis

Sigma1Rs have been shown to associate with diverse proteins, including IP3R, K^+ channel subunit, and BiP[17]. These findings suggest that direct protein interactions may play a role in the functionality of Sigma1R. Recent research indicates that activating Sigma1R can prevent cardiac fibrosis by mitigating impairments in the IRE1α/XBP1 pathway[12,13]. FISH showed partial colocalization between Sigma1R and IRE1α (Fig. 4A). Western blot analysis confirmed strong activation of the IRE1α/XBP1 pathway in AF-treated cells, with increased expression of IRE1α (2.3-fold), phosphorylated IRE1α (1.9-fold), and XBP1s (2.1-fold) relative to controls (Fig. 4B and C). Sigma1R overexpression markedly suppressed these AF-induced changes, indicating inhibition of IRE1α pathway activity. Consistent with the restoration of normal MAM structure, Sigma1R overexpression reduced the expression of key MAM-tethering proteins Grp75, IP_3R, and VDAC1—components that mediate ER-to-mitochondria calcium transfer (Fig. 4D and E). Conversely, IRE1α knockdown produced a similar reduction

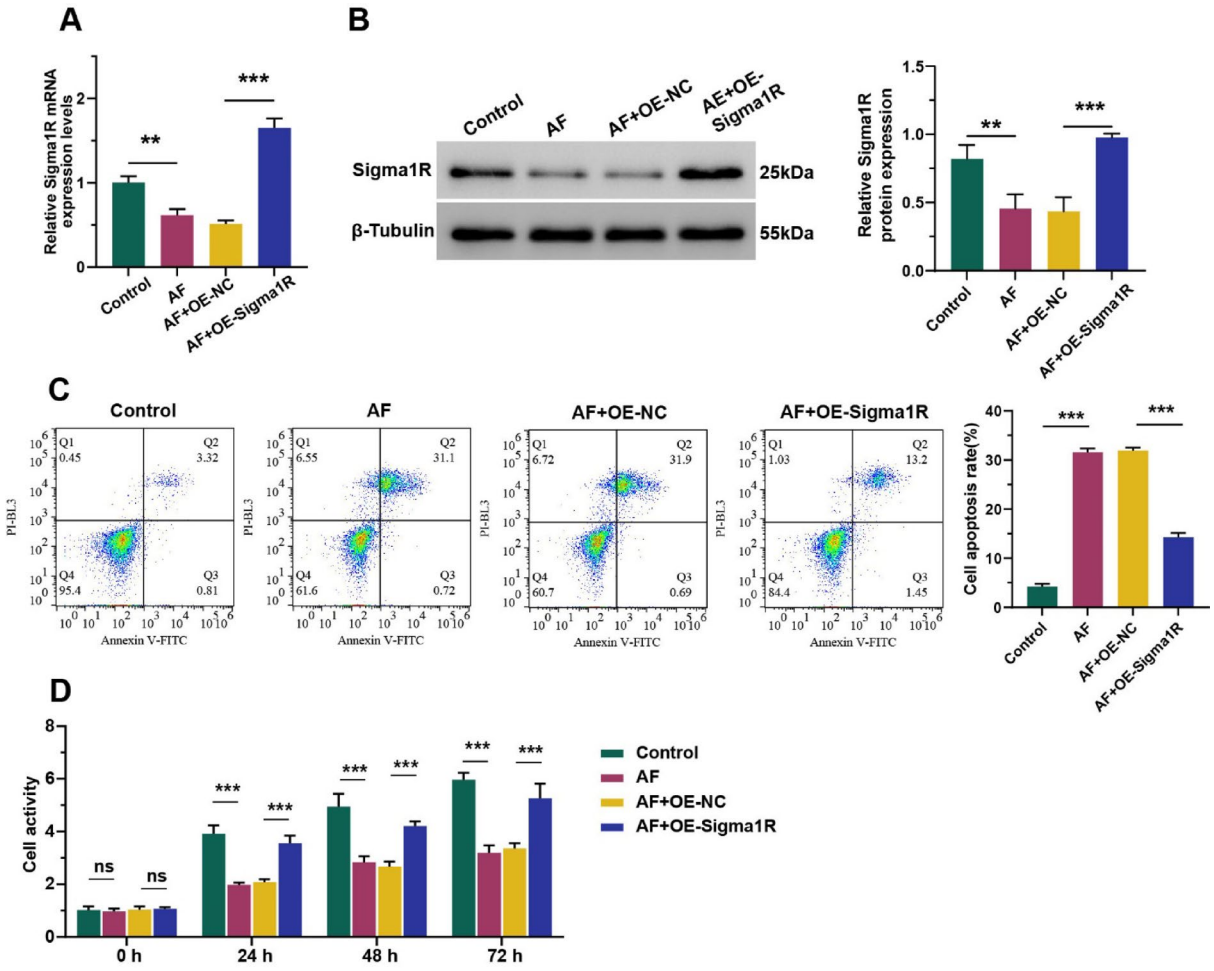

Fig. 1. Sigma1R overexpression inhibits tachypacing-induced damage in atrial myocytes. HL-1 cells were transfected with Sigma1R overexpressing lentivirus (OE-Sigma1R) or control lentivirus (OE-NC), followed by electrical stimulation for 24 h. (**A**) The relative mRNA expression levels of Sigma1R after stimulation (n = 3). (**B**) The relative protein expression levels of Sigma1R after stimulation by WB analysis(n = 3). (**C**) Apoptosis detection was performed with flow cytometry using PI and Annexin V-FITC double staining after stimulation (n = 3). (**D**) CCK-8 assay detected the cell viability after stimulation at 0 h, 24 h, 48 h and 72 h (n = 6). Data are expressed as the mean ± SD. Statistical analysis was performed using one-way ANOVA or two-way ANOVA followed by Tukey's multiple comparisons test. $P^{*} < 0.05$, $P^{**} < 0.01$, $P^{***} < 0.001$.

in these proteins, suggesting that IRE1α drives MAM hyper-tethering and pathological calcium flux, whereas Sigma1R counters this process by suppressing the IRE1α/XBP1 pathway.These findings identify IRE1α/XBP1 as a central mediator of Sigma1R-dependent restoration of calcium homeostasis and MAM organization.

Sigma1R preserves mitochondrial structure and bioenergetic function by suppressing IRE1α

To determine whether the protective effects of Sigma1R on mitochondrial homeostasis depend on IRE1α signaling, HL-1 cells were sequentially transfected with a Sigma1R-overexpression plasmid followed by IRE1α overexpression. As shown in Fig. 5A–D, Sigma1R significantly restored mitochondrial membrane potential (ΔΨm) and reduced mitochondrial ROS levels; however, these improvements were largely reversed when IRE1α was overexpressed, indicating that IRE1α acts downstream of Sigma1R to regulate mitochondrial stress responses. Morphometric analysis of TEM images further supported these findings. As shown in Fig. 5E–H. Sigma1R overexpression increased mitochondrial number, mitochondrial density, and restored MAM contact length toward physiological range, reflecting improved mitochondrial integrity and enhanced MAM organization. In contrast, IRE1α overexpression reduced all three structural parameters, reverting the mitochondrial architecture toward the stressed phenotype observed in AF-treated cells. At the molecular level, Sigma1R overexpression decreased the levels of MAM-associated tethering proteins (Grp75, IP3R, and VDAC1), whereas IRE1α overexpression restored their expression (Fig. 5I and J). Taken together, these results demonstrate that Sigma1R-mediated protection of mitochondrial structure and bioenergetic function is dependent on the suppression of IRE1α signaling and normalization of ER–mitochondria contacts.

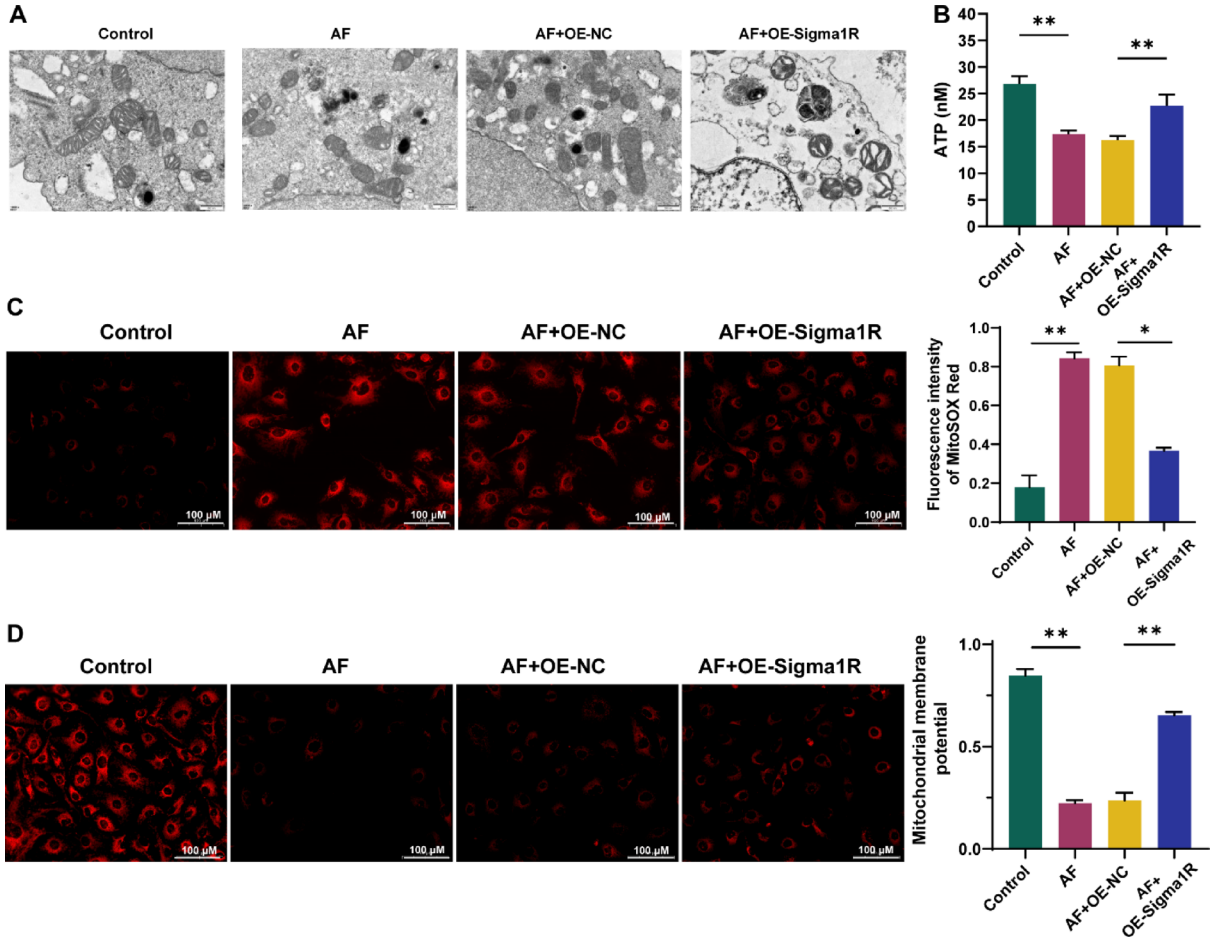

Fig. 2. Sigma1R inhibits tachypacing-induced mitochondrial oxidative stress damage in atrial myocytes. HL-1 cells were transfected with Sigma1R overexpressing lentivirus (OE-Sigma1R) or control lentivirus (OE-NC), followed by electrical stimulation for 24 h. (**A**) Representative transmission electron microscopy images showing mitochondrial morphology in each group (Bar = 500 nm). (**B**) Quantification of ATP levels across different groups (n = 6). (**C**) Representative fluorescence microscopy images depicting mitochondrial superoxide production using MitoSOX Red staining (Bar = 100 μm) and quantification of MitoSOX Red fluorescence intensity (n = 3). (**D**) Representative Mitochondrial membrane potential assessed using fluorescence microscopy (Bar = 100 μm) and quantification of mitochondrial membrane potential across the groups (n = 3). Data are expressed as the mean ± SD. Statistical analysis was performed using one-way ANOVA followed by Tukey's multiple comparisons test. $P^{*} < 0.05$, $P^{**} < 0.01$.

Sigma1R regulates ER–mitochondria calcium flux through the IRE1α/XBP1 pathway

To further characterize the relationship between Sigma1R and IRE1α, we used lentiviral vectors to modulate their expression. Sigma1R overexpression significantly downregulated IRE1α and its active form, phosphorylated IRE1α, whereas IRE1α overexpression increased its own expression and reduced Sigma1R level (Supplementary Fig. 2A and B), suggesting a reciprocal regulatory interaction. Functionally, IRE1α overexpression abolished the cytoprotective effects of Sigma1R on tachypaced cells. Cell viability decreased, apoptosis increased, and ATP production declined when IRE1α was reintroduced into Sigma1R-overexpressing cells (Supplementary Fig. 2C–F). Sigma1R overexpression significantly reduced cytosolic Ca^{2+} overload, but co-expression of IRE1α reversed this effect, linking IRE1α to pathological ER–mitochondria Ca^{2+} flux (Fig. 6A and B). To further evaluate the effects of Sigma1R on ER calcium homeostasis, ER Ca^{2+} content was quantified using a commercial detection kit. Sigma1R also restored ER Ca^{2+} levels in AF-treated cells, whereas IRE1α overexpression reduced ER Ca^{2+} content, reversing Sigma1R's effect (Fig. 6C). Quantitative calcium imaging further confirmed that AF induced robust cytosolic calcium overload, which was significantly reduced by Sigma1R overexpression. However, co-expression of IRE1α abolished the calcium-lowering effect of Sigma1R, increasing cytosolic Ca^{2+} levels to those seen in AF-induced stress (Fig. 6D and E). These data indicate that Sigma1R safeguards mitochondrial energy metabolism under tachypacing stress by suppressing the IRE1α/XBP1 pathway, thereby limiting pathological ER–mitochondria calcium flux and reducing mitochondrial oxidative burden.

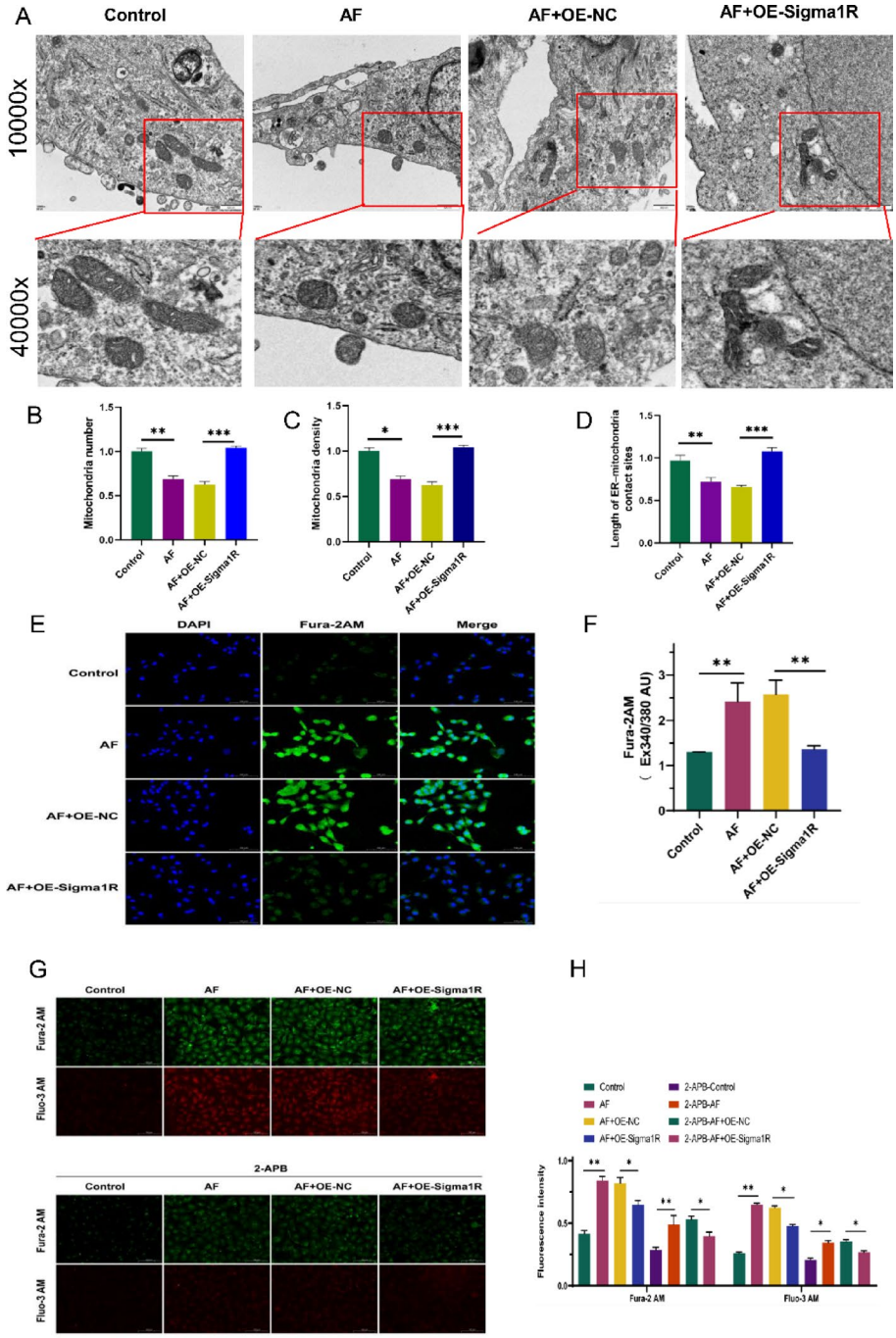

Fig. 3. Sigma1R regulates Ca^{2+} mobilization in MAMs. (**A**) Representative transmission electron microscopy images of mitochondrial ultrastructure in each group (Bar = 500 nm). (**B**) Quantification of mitochondrial number. (**C**) Analysis of mitochondrial density. (**D**) Measurement of ER-mitochondrial contact site length. (**E**) Representative images of immunofluorescence staining using DAPI (nuclei) and Fura-2AM (calcium indicator) (Bar = 100 μm). (**F**) Quantification of Fura-2AM fluorescence intensity (n = 3) of E. (**G**) Representative images of immunofluorescence staining using Fura-2AM (cytosolic calcium indicator) and Fura-3AM (mitochondrial calcium indicator) (Bar = 100 μm). (**H**) Quantification of Fura-2AM or Fura-3AM fluorescence intensity (n = 3). Data are expressed as the mean ± SD. Statistical analysis was performed using one-way ANOVA followed by Tukey's multiple comparisons test. $P^{*} < 0.05$, $P^{**} < 0.01$, $P^{***} < 0.001$.

Discussion

This study highlights the critical role of Sigma1R in protecting atrial myocytes from tachypacing-induced injury by regulating mitochondrial bioenergetics and calcium homeostasis through the IRE1α/XBP1 signaling pathway. Using an *in vitro* model of AF, we show that Sigma1R overexpression significantly improves cell viability and reduces apoptosis, while also enhancing mitochondrial function. These improvements include increased

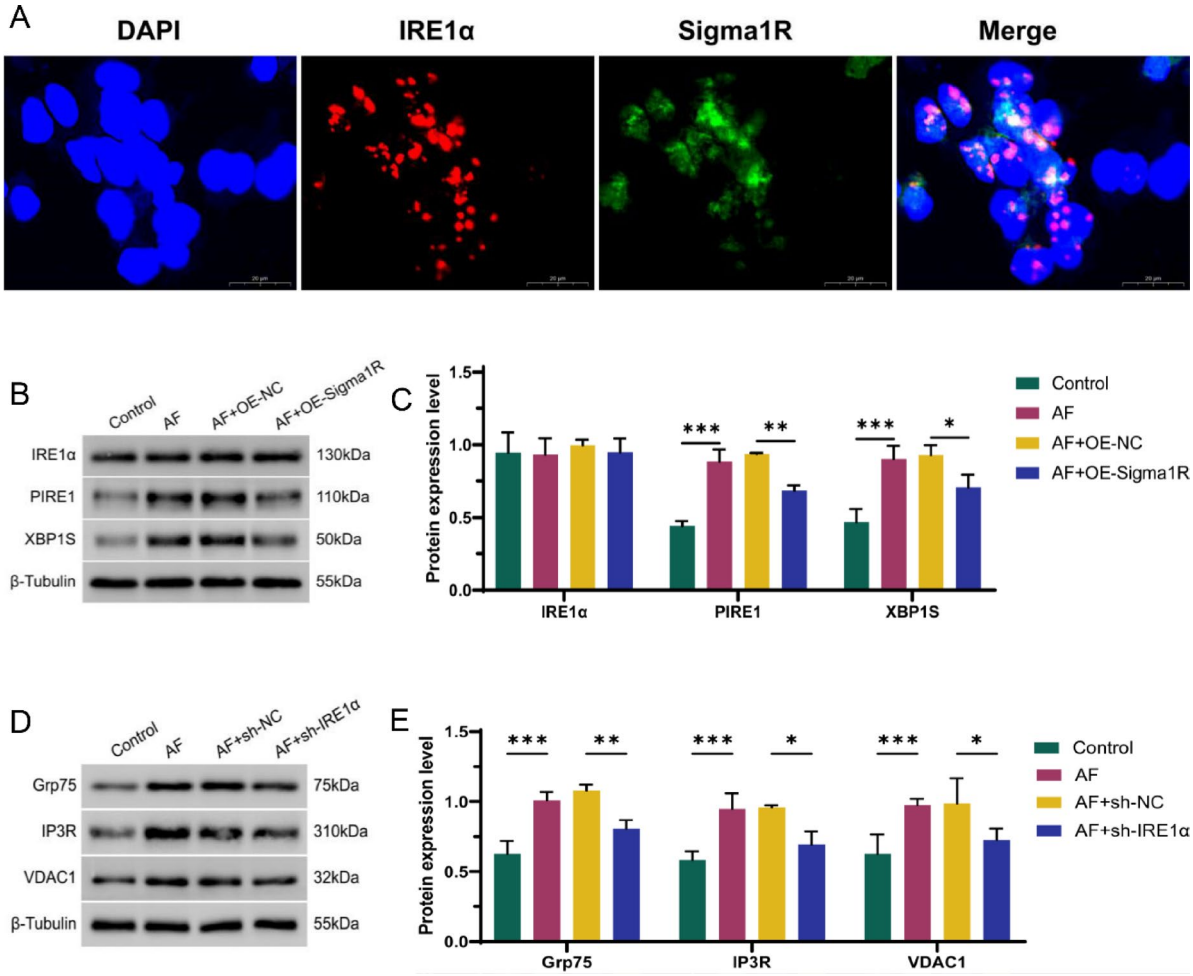

Fig. 4. Sigma1R regulates the Ca^{2+} transport complex on the MAM by targeting the IRE1α/XBP1 axis. (**A**) Fluorescence in situ hybridization images showing the localization of IRE1α (red) and Sigma1R (green) in cells, with DAPI staining the nuclei (blue) (Bar = 20 μm). (**B** and **C**) Western blot analysis of IRE1α, PIRE1, and XBP1S protein levels in each group (n = 3). (**D** and **E**) Western blot analysis of Grp75, IP3R, and VDAC1 in each group (n = 3). Data are expressed as the mean ± SD. Statistical analysis was performed using one-way ANOVA followed by Tukey's multiple comparisons test. $P^{*} < 0.05$, $P^{**} < 0.01$, $P^{***} < 0.001$.

ATP production, decreased mitochondrial ROS levels, and preserved mitochondrial membrane potential. Mechanistically, Sigma1R modulates calcium dynamics at MAMs, reducing cytosolic calcium overload and mitigating mitochondrial calcium accumulation. These findings suggest that Sigma1R plays a protective role in maintaining mitochondrial integrity and function under AF-induced stress by controlling calcium flux through the IRE1α/XBP1 axis.

Mitochondrial dysfunction, characterized by swollen, cristae-disrupted organelles and a 74% decline in membrane potential, is a central pathological feature of our AF model[18]. Sigma1R overexpression countered these structural and functional deficits, maintaining tubular mitochondrial morphology and enhancing ATP generation—critical for sustaining ion channel function and electrical stability, as ATP depletion promotes arrhythmogenesis[7]. The 55% reduction in mitochondrial ROS further underscores Sigma1R's role in attenuating oxidative stress, a known driver of atrial remodeling that exacerbates AF progression[19]. These findings align with Sigma1R's established function as a MAM-localized chaperone that stabilizes ER-mitochondria contacts, ensuring proper calcium transfer essential for oxidative phosphorylation[8,20].

Dysregulated ER-mitochondria calcium signaling is a key node in AF pathogenesis, as evidenced by a significant elevation in cytosolic calcium levels in tachypaced cells[21]. Sigma1R normalized this imbalance through suppression of the IRE1α/XBP1 pathway, which governs the assembly of MAM-localized calcium transporters such as IP3R and Grp75. In AF models, tachypacing induced a 2.1-fold increase in phosphorylated IRE1α (pIRE1α) and a 1.8-fold elevation in XBP1s, markers of excessive unfolded protein response (UPR) activation[22]. The ER and mitochondria are physically and functionally connected through specialized domains called mitochondria-associated ER membranes (MAMs). At MAMs, ER-resident calcium release channels (such as the IP3 receptor, IP3R) form a tight complex with the voltage-dependent anion channel (VDAC) on the mitochondrial outer membrane via molecular chaperone proteins (e.g., GRP75)[23]. This complex constitutes an efficient calcium ion transmission microdomain. Ca^{2+} released from the ER pass directly and rapidly through

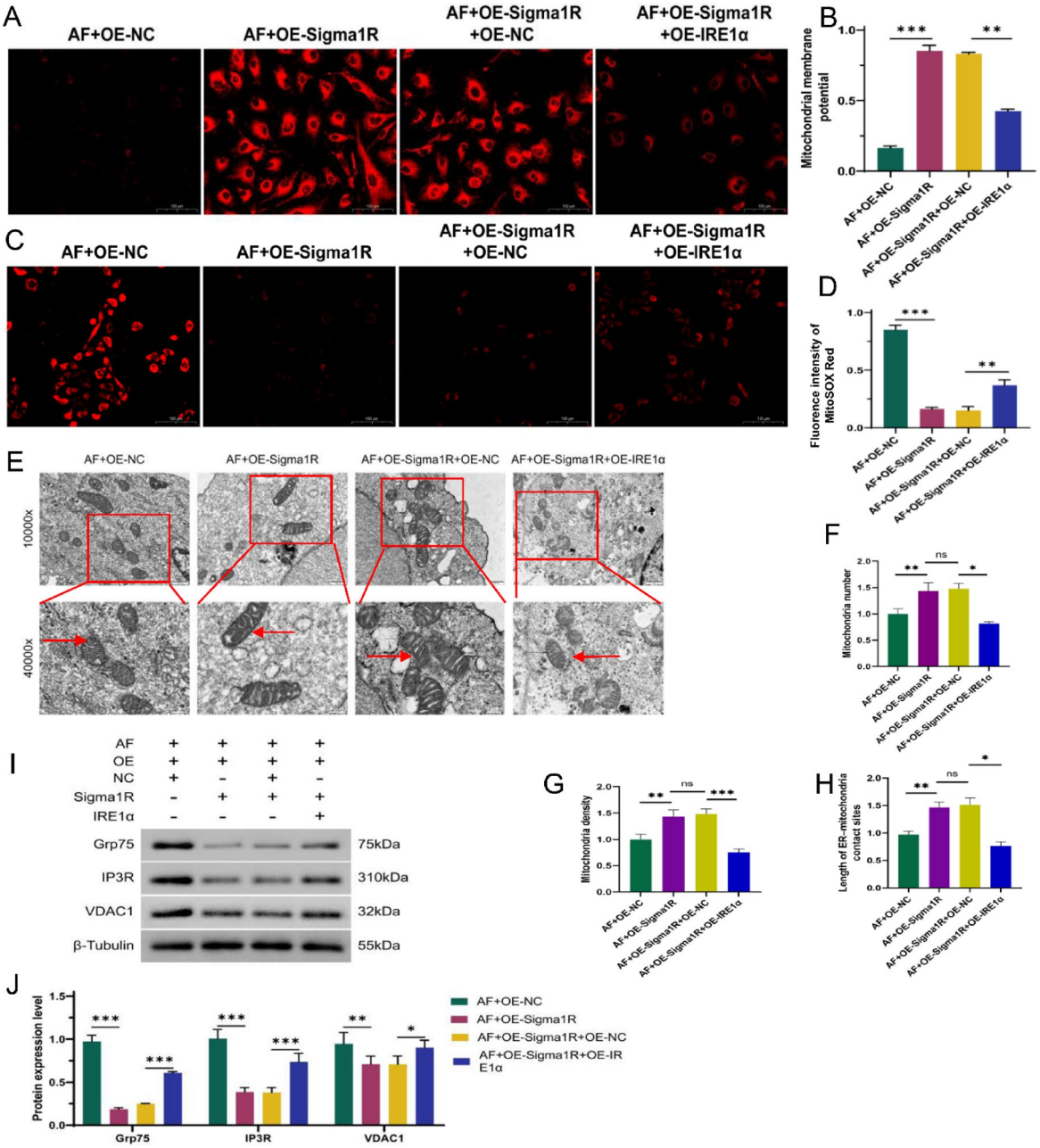

Fig. 5. Effects of Sigma1R and IRE1α on mitochondrial integrity and protein expression in atrial fibrillation. (**A**) Representative Mitochondrial membrane potential assessed using fluorescence microscopy (Bar = 100 μm). (**B**) Quantification of mitochondrial membrane potential across the groups (n = 3). (**C**) Representative fluorescence microscopy images depicting mitochondrial superoxide production using MitoSOX Red staining (Bar = 100 μm). (**D**) Quantification of MitoSOX Red fluorescence intensity (n = 3). (**E**) Representative transmission electron microscopy images of mitochondrial ultrastructure in each group (Bar = 500 nm), the red arrow indicates the mitochondria. (**F**) Quantification of mitochondrial number. (**G**) Analysis of mitochondrial density. (**H**) Measurement of ER-mitochondrial contact site length. (**I** and **J**) Western blot analysis of Grp75, IP3R, and VDAC1 in each group (n = 3). Data are expressed as the mean ± SD. Statistical analysis was performed using one-way ANOVA followed by Tukey's multiple comparisons test. $P^{*} < 0.05$, $P^{**} < 0.01$, $P^{***} < 0.001$.

this complex into the mitochondrial matrix, which is driven by the mitochondrial membrane potential. This localized high-concentration calcium flux serves as the primary physiological signal for activating key dehydrogenases within the mitochondrial matrix (such as the pyruvate dehydrogenase complex, α-ketoglutarate dehydrogenase, and isocitrate dehydrogenase)[24]. This activation drives the tricarboxylic acid (TCA) cycle and oxidative phosphorylation (OXPHOS) to produce ATP. However, when this calcium signaling regulation is disrupted—whether due to sustained increases in ER calcium release (e.g., potent or persistent agonist

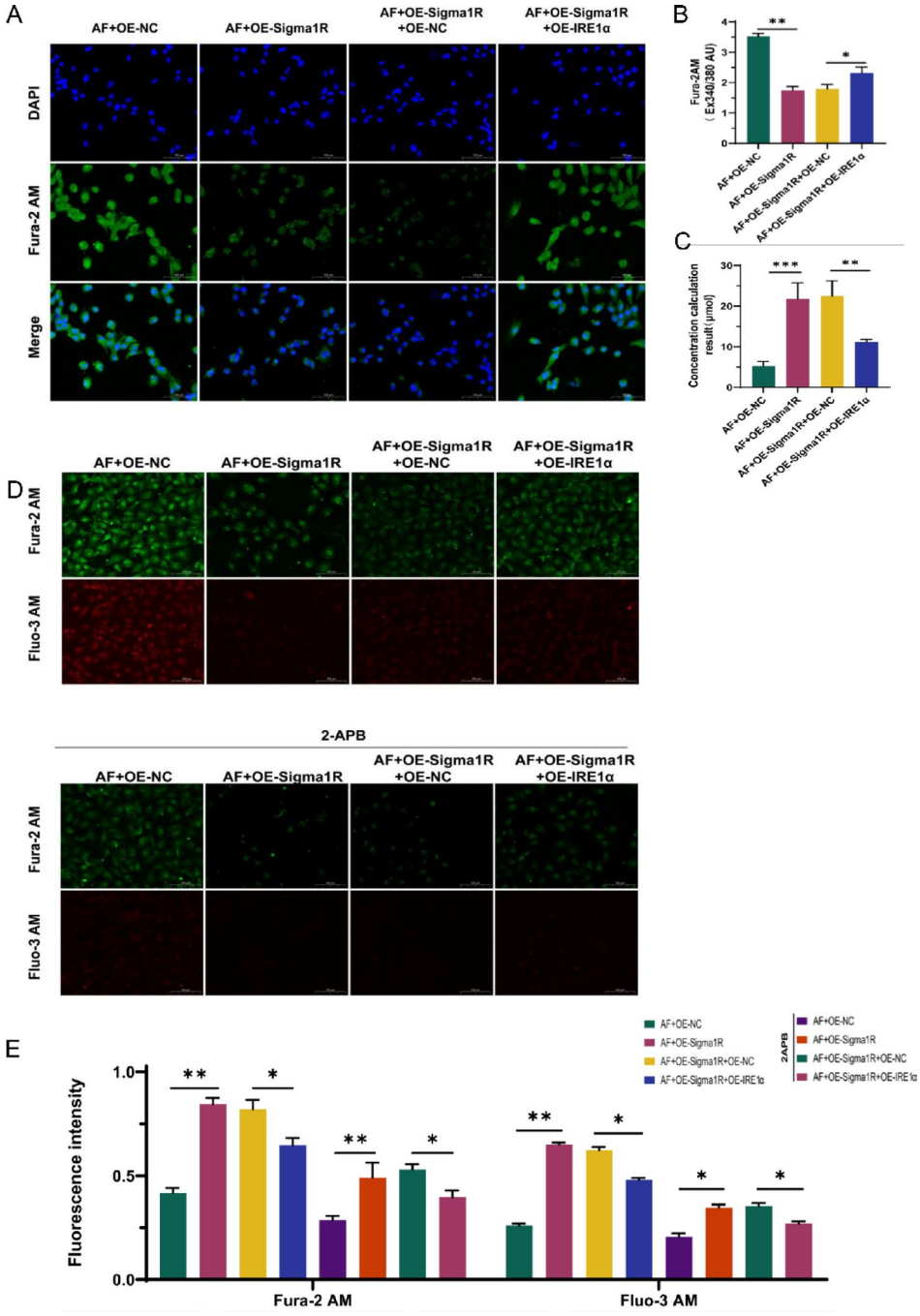

Fig. 6. Regulation of calcium homeostasis by Sigma1R and IRE1α in atrial fibrillation. (**A**) Representative images of immunofluorescence staining using DAPI (nuclei) and Fura-2AM (calcium indicator) (Bar = 100 μm). (**B**) Quantification of Fura-2AM fluorescence intensity (n = 3). (**C**) Quantification of Ca^{2+} in the endoplasmic reticulum (n = 6). (**D**) Representative images of immunofluorescence staining using Fura-2AM (cytosolic calcium indicator) and Fura-3AM (mitochondrial calcium indicator) (Bar = 100 μm). (**E**) Quantification of Fura-2AM or Fura-3AM fluorescence intensity (n = 3). Data are expressed as the mean ± SD. Statistical analysis was performed using one-way ANOVA followed by Tukey's multiple comparisons test. $P^{*} < 0.05$, $P^{**} < 0.01$, $P^{***} < 0.001$.

stimulation, ER stress), structural abnormalities in MAMs (e.g., dysregulation in the expression, localization, or interaction of linker proteins like IP3R/VDAC, or defects in regulatory proteins such as Mfn2, PACS-2, Fis1), or reduced mitochondrial calcium buffering/efflux capacity—it leads to mitochondrial calcium overload. Excess calcium ions induce the uncontrolled opening of the mitochondrial permeability transition pore (mPTP), which disrupts the mitochondrial membrane potential. This results in interrupted ATP synthesis, a burst of reactive oxygen species (ROS) production, and ultimately triggers the release of pro-apoptotic factors like cytochrome

c, initiating the cell apoptosis program. Furthermore, dysregulated calcium signaling also impairs ER calcium homeostasis itself, exacerbating ER stress and the unfolded protein response (UPR), creating a vicious cycle. Thus, calcium ion signaling at MAMs is a core function; its precise regulation is crucial for maintaining cellular energy metabolism and survival[25]. Dysregulation of this pathway is a key mechanism underlying various pathological states, including neurodegenerative diseases, metabolic diseases, cardiovascular diseases, and cancer. Sigma1R overexpression significantly reduced the responses associated with calcium overload, as evidenced by decreased IP3R and Grp75 expression in IRE1α-knockdown cells. The IP3R antagonist 2-APB mirrored Sigma1R's calcium-lowering effects, supporting the hypothesis that Sigma1R prevents calcium overload by regulating this crucial shuttle mechanism, which otherwise activates pro-apoptotic mitochondrial pathways and impairs bioenergetics[26,27].

Genetic rescue experiments provided further evidence for the IRE1α/XBP1 pathway as a downstream effector of Sigma1R: IRE1α overexpression abolished Sigma1R-mediated protection, reducing cell viability and increasing apoptosis, while reversing ATP recovery. Mechanistically, IRE1α overexpression exacerbated mitochondrial structural damage, increasing cristae disruption and upregulating Grp75/IP3R/VDAC1 complexes, enhancing calcium transfer and mitochondrial stress. These data establish a direct link between Sigma1R-IRE1α interaction and MAM calcium flux regulation, highlighting the IRE1α/XBP1 axis as a critical mediator of Sigma1R's protective effects. Sigma1R overexpression normalized calcium flux, suggesting its role in preventing calcium overload, a known contributor to mitochondrial dysfunction and AF pathogenesis[28]. These effects were further supported by experiments with the IP3 receptor antagonist 2-APB, which demonstrated that Sigma1R modulates ER-mitochondria calcium transfer through the regulation of calcium transport proteins, including Grp75, IP3R, and VDAC1[29]. This finding aligns with Sigma1R's known function as a molecular chaperone at MAMs, ensuring proper calcium signaling and mitochondrial function. Upon ER stress, the Sigma1R dissociates from BiP which also is known to dissociate from IRE1, upon the same stress[13,30]. The Sigma1R molecular chaperone enhances its association with IRE1 to correct or stabilize the conformation of IRE1 to regulate cellular survival by attenuating ER stress[31,32]. Sigma1R overexpression attenuated the upregulation of IRE1α and its downstream effectors, PIRE1 and XBP1S, in tachypaced myocytes. Importantly, overexpression of IRE1α abolished Sigma1R's protective effects, leading to increased apoptosis, mitochondrial dysfunction, and calcium dysregulation. This suggests that Sigma1R's protective role involves inhibiting excessive activation of the IRE1α/XBP1 axis, thereby mitigating calcium overload and maintaining mitochondrial integrity. This mechanistic insight expands on previous studies linking IRE1α/XBP1 dysregulation to cardiac pathophysiology and underscores the therapeutic potential of targeting this pathway.

While our findings demonstrate that Sigma1R reduces mitochondrial ROS in atrial myocytes, this appears to contrast with previous reports in neuronal systems, where pharmacological activation of Sigma1R has been associated with increased ROS production[33]. These divergent observations likely reflect cell-type–specific differences in Sigma1R function as well as distinct modes of activation (genetic overexpression versus acute pharmacological stimulation). In atrial myocytes, the enrichment of Sigma1R at mitochondria-associated membranes may favor calcium buffering and ER–mitochondria communication rather than ROS-generating signaling pathways, highlighting the importance of context-dependent mechanisms. Several limitations should be acknowledged. First, our experiments were performed in vitro using murine HL-1 atrial myocytes, which, despite retaining cardiomyocyte-like features, do not fully recapitulate the electrophysiological or contractile properties of mature human atrial cells. Second, Ca^{2+} transient measurements—while highly informative for excitation–contraction coupling—were not included in this study due to the specialized instrumentation required. Nevertheless, these limitations do not affect the core conclusions of our work, which center on mitochondrial bioenergetics, ER–mitochondria crosstalk, and Sigma1R-mediated regulation of the IRE1α/XBP1 pathway. Future studies employing primary human atrial myocytes and in vivo AF models will be essential to validate the translational relevance of Sigma1R signaling and to determine how long-term Sigma1R activation influences atrial remodeling and electrophysiological stability.

Conclusion

In conclusion, this work establishes Sigma1R as a key regulator of mitochondrial energy metabolism in AF, operating through inhibition of the IRE1α/XBP1 pathway to normalize MAM calcium transport and suppress ER stress. By bridging ER-mitochondria crosstalk, Sigma1R protects against tachypacing-induced bioenergetic failure and cell death, offering a promising therapeutic target to address the unmet need for interventions that tackle both electrical and metabolic remodeling in AF.

Data availability

All data generated or analysed during this study are included in this published article and its supplementary information files.

Received: 21 May 2025; Accepted: 3 December 2025
Published online: 20 December 2025

References

1. Middeldorp, M. E., Kamsani, S. H. & Sanders, P. Obesity and atrial fibrillation: Prevalence, pathogenesis, and prognosis. *Prog. Cardiovasc. Dis.* **78**, 34–42 (2023).
2. Ahmadzadeh, K., Hajebi, A., Adel Ramawad, H., Azizi, Y. & Yousefifard, M. Value of N-terminal pro-brain natriuretic peptide for embolic events risk prediction in patients with atrial fibrillation; a systematic review and meta-analysis. *Arch. Acad. Emerg. Med.* **11**(1), e8 (2023).

3. Chyou, J. Y. *et al.* Atrial fibrillation occurring during acute hospitalization: A scientific statement from the American Heart Association. *Circulation* **147**(15), e676–e698 (2023).
4. Brundel, B., Ai, X., Hills, M. T., Kuipers, M. F., Lip, G. Y. H., de Groot, N. M. S. Atrial fibrillation. *Nature Reviews. Disease Primers* **8**(1), 21 (2022)
5. Werbner, B., Tavakoli-Rouzbehani, O. M., Fatahian, A. N. & Boudina, S. The dynamic interplay between cardiac mitochondrial health and myocardial structural remodeling in metabolic heart disease, aging, and heart failure. *J. Cardiovasc. Aging* **3**(1), 9 (2023).
6. Pool, L., Wijdeveld, L., de Groot, N. M. S. & Brundel, B. The role of mitochondrial dysfunction in atrial fibrillation: Translation to druggable target and biomarker discovery. *Int. J. Mol. Sci.* **22**(16), 8463 (2021).
7. Mason, F. E., Pronto, J. R. D., Alhussini, K., Maack, C. & Voigt, N. Cellular and mitochondrial mechanisms of atrial fibrillation. *Basic Res. Cardiol.* **115**(6), 72 (2020).
8. Voronin, M. V., Abramova, E. V., Verbovaya, E. R., Vakhitova, Y. V. & Seredenin, S. B. Chaperone-dependent mechanisms as a pharmacological target for neuroprotection. *Int. J. Mol. Sci.* **24**(1), 823 (2023).
9. Missiroli, S. *et al.* Mitochondria-associated membranes (MAMs) and inflammation. *Cell Death Dis.* **9**(3), 329 (2018).
10. Ye, T. *et al.* Chronic inhibition of the sigma-1 receptor exacerbates atrial fibrillation susceptibility in rats by promoting atrial remodeling. *Life Sci.* **235**, 116837 (2019).
11. Zhou, L., Zhu, X., Lei, S., Wang, Y. & Xia, Z. The role of the ER stress sensor IRE1 in cardiovascular diseases. *Mol. Cell Biochem.* **480**(2), 683–691 (2025).
12. Hayashi, T. & Su, T. P. Sigma-1 receptor chaperones at the ER-mitochondrion interface regulate Ca(2+) signaling and cell survival. *Cell* **131**(3), 596–610 (2007).
13. Mori, T., Hayashi, T., Hayashi, E. & Su, T. P. Sigma-1 receptor chaperone at the ER-mitochondrion interface mediates the mitochondrion-ER-nucleus signaling for cellular survival. *PLoS ONE* **8**(10), e76941 (2013).
14. Liu, X. *et al.* Chronic stimulation of the sigma-1 receptor ameliorates autonomic nerve dysfunction and atrial fibrillation susceptibility in a rat model of depression. *Am. J. Physiol. Heart Circ. Physiol.* **315**(6), H1521-h1531 (2018).
15. Wiersma, M. *et al.* Cell-free circulating mitochondrial DNA: A potential blood-based marker for atrial fibrillation. *Cells* **9**(5), 1159 (2020).
16. Liu, X. *et al.* The reversal effect of sigma-1 receptor (S1R) agonist, SA4503, on atrial fibrillation after depression and its underlying mechanism. *Front. Physiol.* **10**, 1346 (2019).
17. Hayashi, T. & Su, T. P. Regulating ankyrin dynamics: Roles of sigma-1 receptors. *Proc. Natl. Acad. Sci. U.S.A.* **98**(2), 491–496 (2001).
18. Deng, J. *et al.* Mitochondrial dysfunction in cardiac arrhythmias. *Cells* **12**(5), 679 (2023).
19. Brailoiu, E. *et al.* Modulation of the blood-brain barrier by sigma-1R activation. *Int. J. Mol. Sci.* **25**(10), 5147 (2024).
20. Wang, J. *et al.* Sigma 1 receptor regulates the oxidative stress response in primary retinal Müller glial cells via NRF2 signaling and system xc(-), the Na(+)-independent glutamate-cystine exchanger. *Free Radic. Biol. Med.* **86**, 25–36 (2015).
21. Lattanzio, F. A. Jr. *et al.* Cocaine increases intracellular calcium and reactive oxygen species, depolarizes mitochondria, and activates genes associated with heart failure and remodeling. *Cardiovasc. Toxicol.* **5**(4), 377–390 (2005).
22. Munguia-Galaviz, F. J., Miranda-Diaz, A. G., Cardenas-Sosa, M. A. & Echavarria, R. Sigma-1 receptor signaling: In search of new therapeutic alternatives for cardiovascular and renal diseases. *Int. J. Mol. Sci.* **24**(3), 1997 (2023).
23. Mao, H., Chen, W., Chen, L. & Li, L. Potential role of mitochondria-associated endoplasmic reticulum membrane proteins in diseases. *Biochem. Pharmacol.* **199**, 115011 (2022).
24. Jiang, R. Q., Li, Q. Q. & Sheng, R. Mitochondria associated ER membranes and cerebral ischemia: Molecular mechanisms and therapeutic strategies. *Pharmacol. Res.* **191**, 106761 (2023).
25. Zhao, W. B. & Sheng, R. The correlation between mitochondria-associated endoplasmic reticulum membranes (MAMs) and Ca(2+) transport in the pathogenesis of diseases. *Acta Pharmacol. Sin.* **46**(2), 271–291 (2025).
26. Zheng, D. *et al.* ROS-triggered endothelial cell death mechanisms: Focus on pyroptosis, parthanatos, and ferroptosis. *Front. Immunol.* **13**, 1039241 (2022).
27. Zhang, D. *et al.* Mitochondrial cardiomyopathy caused by elevated reactive oxygen species and impaired cardiomyocyte proliferation. *Circ. Res.* **122**(1), 74–87 (2018).
28. Denham, N. C. *et al.* Calcium in the pathophysiology of atrial fibrillation and heart failure. *Front. Physiol.* **9**, 1380 (2018).
29. Yuan, M. *et al.* IP3R1/GRP75/VDAC1 complex mediates endoplasmic reticulum stress-mitochondrial oxidative stress in diabetic atrial remodeling. *Redox. Biol.* **52**, 102289 (2022).
30. Kim, M. & Bezprozvanny, I. Structure-based modeling of sigma 1 receptor interactions with ligands and cholesterol and implications for its biological function. *Int. J. Mol. Sci.* **24**(16), 12980 (2023).
31. Qu, J. *et al.* Stimulation of sigma-1 receptor protects against cardiac fibrosis by alleviating IRE1 pathway and autophagy impairment. *Oxid. Med. Cell. Longev.* **2021**, 8836818 (2021).
32. Rosen, D. A. *et al.* Modulation of the sigma-1 receptor-IRE1 pathway is beneficial in preclinical models of inflammation and sepsis. *Sci. Transl. Med.* **11**(478), eaau5266 (2019).
33. Goguadze, N., Zhuravliova, E., Morin, D., Mikeladze, D. & Maurice, T. Sigma-1 receptor agonists induce oxidative stress in mitochondria and enhance complex I activity in physiological condition but protect against pathological oxidative stress. *Neurotox. Res.* **35**(1), 1–18 (2019).

Acknowledgements

The authors express their appreciation to staff in Affiliated Hospital of Youjiang Medical University for Nationalities and Wuzhou People's Hospital, for their technical assistance.

Author contributions

Conceptualization: Wei Yan, Zhile Li; Data curation: Tongyuan Deng, Da Huang, Bailu Deng, Hong Ling; Formal analysis: Wei Yan, Tongyuan Deng, Da Huang, Bailu Deng, Hong Ling, Zhile Li; Investigation: Tongyuan Deng, Da Huang, Bailu Deng, Hong Ling; Writing—original draft: Wei Yan, Tongyuan Deng, Da Huang, Bailu Deng, Hong Ling; Writing—review and editing: Wei Yan, Zhile Li.

Declarations

Competing interests

The authors declare no competing interests.

Additional information

Supplementary Information The online version contains supplementary material available at https://doi.org/1

0.1038/s41598-025-31500-5.

Correspondence and requests for materials should be addressed to Z.L.